Molecular dynamics of a water jet from a carbon nanotube

Itsuo Hanasaki,* Toru Yonebayashi, and Satoyuki Kawano†
Department of Mechanical Science and Bioengineering, Graduate School of Engineering Science, Osaka University, Machikaneyama-cho 1-3, Toyonaka, Osaka 560-8531, Japan
(Received 17 November 2008; published 6 April 2009)

A carbon nanotube (CNT) can be viewed as a molecular nozzle. It has a cylindrical shape of atomistic regularity, and the diameter can be even less than 1 nm. We have conducted molecular-dynamics simulations of water jet from a (6,6) CNT that confines water in a form of single-file molecular chain. The results show that the water forms nanoscale clusters at the outlet and they are released intermittently. The jet breakup is dominated by the thermal fluctuations, which leads to the strong dependence on the temperature. The cluster size n decreases and the release frequency f increases at higher temperatures. The f roughly follows the reaction kinetics by the transition state theory. The speed of a cluster is proportional to the $1/\sqrt{n}$ because of the central limit theorem. These properties make great contrast with the macroscopic liquid jets.

DOI: 10.1103/PhysRevE.79.046307 PACS number(s): 47.61.Fg, 47.60.Kz

I. INTRODUCTION

The concept of nanojet has been used in theoretical [1–5] and experimental [6–9] studies in recent years. This is a novel realm of nanoscale fluid dynamics of profound engineering relevance as well as of pure scientific significance. It has become a realistic subject owing to the advances of micromachining in the field of microelectromechanical/nanoelectromechanical systems (MEMS/NEMS). Hence, they are usually supposed to be produced by so-called top-down process, i.e., manufactured from larger pieces of materials. It is extremely difficult to obtain a cylindrical material with a diameter of a few nanometers with atomistic precision of the shape if the production relies on the top-down process.

However, there are such materials already in reality: the carbon nanotubes (CNTs) [10,11]. They are molecules of cylindrical shape with atomistically smooth surface. They have even mechanical strength and wear resistance, which is crucial for engineering use especially for the applications as nanochannels. In recent years, studies of nanofluidic applications of CNTs have been extensively conducted: fluid properties inside CNTs in equilibrium [12–22], intermittent fluid conduction through CNT immersed in equilibrium water [20], and steady-state flow inside CNTs [23–25]. There have been not only theoretical/computational predictions of phenomena but also experimental reports of the transport characteristics [26]. The theoretical predictions [23–25] and experimental observation [26] of the flow through CNT agrees in that it is different from Poiseuille flow through a macroscopic cylindrical channel while the detail still has room for discussion.

In this study, we regard a CNT as a nozzle, and conduct molecular-dynamics (MD) simulations to elucidate the nanojet properties that can be substantially different from the macroscopic ones. In spite of much attention to the CNTs mentioned above, there have been no reports that treat a CNT as a nozzle that realizes nanojets as the authors envision. Jets have long been utilized in various situations such as propulsion, actuation, processing (e.g., cutting), cooling/heating, and mixing. When the nozzle is nanoscale, there will be the corresponding applications for MEMS/NEMS, control of chemical reactions, and microsurgery for medical purpose. Furthermore, the understanding of nanojet is also important as it is a challenge to control the motion of molecules. In this paper, we focus on the water jet properties from a (6,6) CNT. The (6,6) CNT, having the diameter of 0.81 nm, has been reported to have special characteristics compared to other CNTs with larger diameters [20–22]. The confined water forms single-file chain structure. The chain comprised of water molecules has hydrogen bonds between the adjacent molecules. Thus, the (6,6) CNT can be one of the smallest channels that conduct water. Therefore, we specify the molecular species explicitly although the characteristics found in this study are expected to be general to some extent. This is in contrast with the previous studies that focus on liquid threads [27–29], where Lennard-Jones fluids are used for model generality. In this study, the specification is important for the foundation of the system properties such as single-file conduction of water with hydrogen bonds. We expect that similar phenomena occur if some necessary conditions are satisfied but our model specification clarifies the realistic system that is the most promising at the moment.

II. MODEL AND METHODS

We consider the system consisting of water and CNT. Both of them are modeled as rigid molecules. We use SPC/E model [30] for water, and we fix the carbon atoms of the CNT in space. The rigid treatment of the CNT for nanofluidic studies using MD is widely accepted [19,21,23–25,31–33] although it does not necessarily mean that there is no difference between rigid and flexible models [34,35]. We use the rigid CNT model since our focus in this paper is the qualitative discussion and the flexible model needs shorter time step that substantially increases the computational cost. It has been reported that the water flow through the (6,6) CNT is intermittent and pulselike [20]. This

*hanasaki@me.es.osaka-u.ac.jp
†kawano@me.es.osaka-u.ac.jp

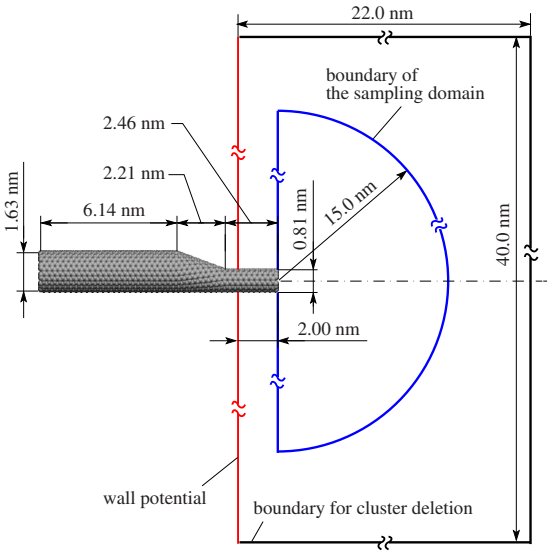

FIG. 1. (Color online) Schematic view of the computational model.

originates from the kinetics and energetics at the entrance of the CNT surrounded by liquid water. It is a subtle condition, and might be altered by the different terminations of the CNT edge. Hence, the inlet conditions can be diverse, and one of the possible situations should be specified. Since we intend to compare the jet properties with well-established macroscopic ones, the continuous supply of the work fluid from the upstream is desirable. It is still not certain whether it can be realized with the pure (6,6) CNT but we consider it reasonable to assume that it is possible if the channel width in the upstream is wide enough. There is a structure in reality that consists of two nanotubes having different diameters connected with each other seamlessly, which are called CNT junctions [36,37]. In the previous study, we reported convergent nozzle properties of CNT junctions using MD [38]. In this paper, we use the (12,12)-(6,6) CNT junction to realize the continuous water supply from the upstream.

The system configuration is schematically illustrated in Fig. 1. The diameters of the (12,12) and (6,6) CNTs are 1.63 and 0.81 nm, and their lengths are defined as 6.14 and 2.46 nm, respectively. The length of the junction part is 2.21 nm. In order to induce the continuous flow through the upstream wide CNT and consequently the downstream (6,6) CNT, we use fluidized piston model (FPM) [39]. It enables the flow through nonuniform geometry in MD by applying adaptive external field to the fluid only in the specific localized domain in the upstream that is located away from the domain of interest. No periodic boundary condition is applied in the domain. The temperature control is another issue when a driving force exists but it is also applied only outside the domain of interest during the sampling. Such conditions are suitable for this study. The fluidized piston region of the FPM, which acts both as a piston to press the fluid downstream and the fluid reservoir, is located in the upstream end with a length of 4.91 nm in the (12,12) CNT.

The potential function consists of Lennard-Jones $\phi_{\mathrm{LJ}}(r_{ij})$ and electrostatic $\phi_E(r_{ij})$ interactions as follows:

$$\phi_{\mathrm{LJ}}(r_{ij}) = 4\varepsilon\left[\left(\frac{\sigma}{r_{ij}}\right)^{12} - \left(\frac{\sigma}{r_{ij}}\right)^{6}\right], \tag{1}$$

$$\phi_E(r_{ij}) = \frac{1}{4\pi\varepsilon_0}\left[\frac{q_i q_j}{r_{ij}} - E_s(r_{ij})\right], \tag{2}$$

$$E_s(r_{ij}) = \frac{q_i q_j}{r_c} - (r_{ij} - r_c)\frac{q_i q_j}{r_c^2}, \tag{3}$$

where r_{ij} is the distance between the atoms i and j. The Lennard-Jones potential is considered between oxygen atoms, and between oxygen and carbon atoms. Coulomb potential is considered between every atomic pair between water molecules. Using the smooth cutoff scheme for Coulomb interactions, all the nonbonded interactions are cut off at 1 nm. This is a reasonable choice of the treatment of electrostatic interactions because the system we study here is not a bulk system or that with periodic boundary conditions. Ewald summation is not compatible with such conditions. As shown in Fig. 1, the wall potential is located at the upstream end of the (12,12) CNT and around the (6,6) CNT at 2.00 nm distance in the upstream direction from the outlet [39]. The potential parameters $\sigma, \varepsilon, \varepsilon_0$, and q_i used in this study are the same as Refs. [21,39]. The simulation domain for the jet has a length of 22.0 nm in the downstream direction, and a radius of 20.0 nm in the perpendicular direction, which forms the cylindrical shape. The whole cluster of water molecules are removed from the domain when one of the constituent atoms goes out of it. A pair of water molecules is defined to be in the same cluster if the distance of the oxygen atom of one molecule is less than 3.6 Å from that of the other molecule. The value of 3.6 Å is one of the necessary conditions often used for the conventional definition of hydrogen bonds between water molecules in MD [12,21,25]. This value is related to the first minima of the radial distribution function for the oxygen atoms of water [40].

We solve the equations of motion using the velocity Verlet algorithm with a time step of 2 fs. The RATTLE algorithm [43] is applied to the rigid water model. 600 molecules of water are located in the CNT junction at the beginning of the simulation. The temperature is controlled by velocity scaling in the directions perpendicular to the flow. It is applied to the whole system only for the first 50 ps. After that period, the temperature is controlled only inside the fluidized piston region. As the simulation proceeds, the number of water molecules inside the fluidized piston region decreases. The density there is maintained in the range from 30 to 45 molecules/nm^3 by insertion and deletion of the water molecules. In the original FPM, the water that went out of the downstream end was recycled and the total number of molecules was constant. In this study, it is not constant. The sampling of the jet properties are conducted for 5000 ps after the 2000 ps of preliminary simulation after the first 50 ps. The total simulation time is thus 7050 ps. Since this study focuses on qualitative trend rather than the prediction of the specific numerical values, the sampling is conducted until the influences of the temperature on the jet properties are clearly observed. The inlet velocities of 0.5, 1.0, and 2.0 m/s at

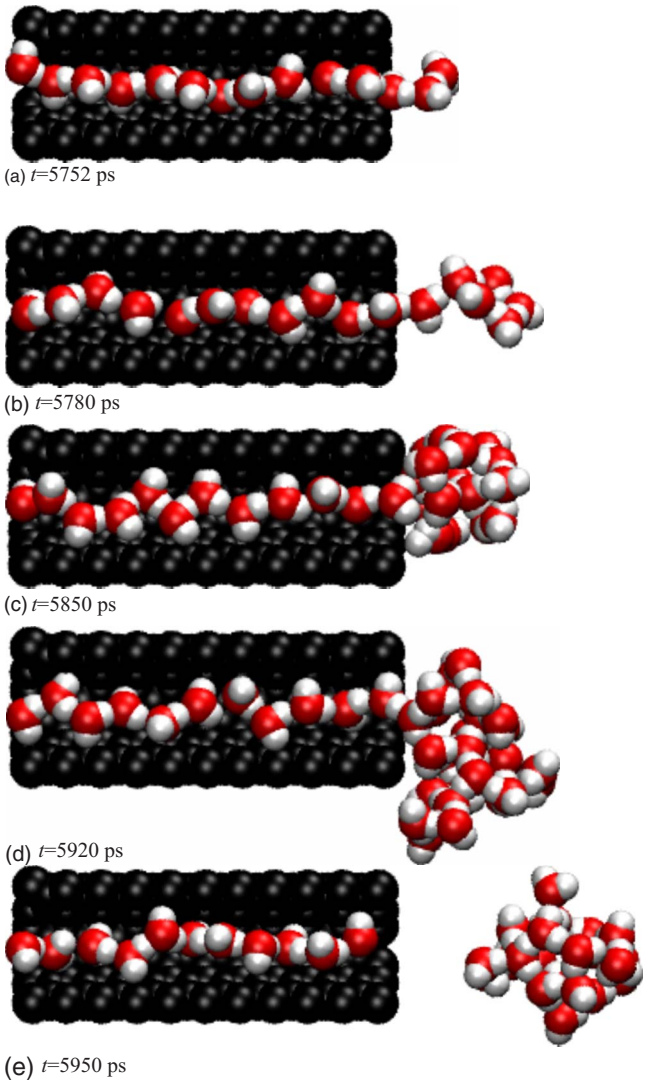

FIG. 2. (Color online) Sequential snapshots of water jet from the (6,6) CNT, where the outlet streaming velocity and temperature are 24 m/s and 341 K, respectively.

different inlet temperatures of 300, 350, 400, 450, and 500 K lead to the average outlet velocities u_{out} of 9 ± 3.9, 13 ± 1.1, and 23 ± 0.9 m/s, respectively, where the values after "±" indicate the standard deviations. The outlet velocities are measured in the domain with a length of 1 nm along the tube axis inside the (6,6) CNT from the edge. The outlet temperature is defined in the same region using the variation in the translational velocities of the molecules. In what follows, the outlet velocity is used for the identification of each case in the figures. It should be noted that u_{out} is different from the speed of the jet because the former is measured inside the nozzle and the latter has unique characteristics as we discuss in the following.

III. RESULTS AND DISCUSSION

A. Elementary process and the energetics

One of the typical jet dynamics is shown in Fig. 2, where the flow direction is from left to right. Visual molecular dynamics (VMD) [41] is used for the visualization of molecules. It can be seen from Fig. 2 that the single-file water molecules form a cluster or a nanoscale droplet at the outlet. The cluster size grows there for some period of time, then it is released from the outlet. Within the range discussed here, the flow of the water jet is mainly an intermittent cluster release phenomenon. The cluster can be considered to be released from the outlet region when the following condition is satisfied,

$$\frac{1}{2} m_{\text{cls}} \boldsymbol{u}_{\text{cls}}^2 - (\Delta E_{\text{cluster-CNT}} + \Delta E_{\text{cluster-chain}}) > 0, \qquad (4)$$

where m_{cls} and $\boldsymbol{u}_{\text{cls}}$ are the mass and velocity of the cluster getting released, $\Delta E_{\text{cluster-CNT}}$ and $\Delta E_{\text{cluster-chain}}$ are the binding energies between the cluster and CNT, and that between the cluster and the upstream water chain connected to it. The cluster can sometimes be already ruptured from the upstream chain inside the (6,6) CNT. In that case, the necessary kinetic energy for the cluster release is smaller by $\Delta E_{\text{cluster-chain}}$ than that in the situation shown in Fig. 2.

In order to clarify the energetics of this process, we examined the binding energies between the CNT edge and water, and that between the water molecules. We calculated the state of the minimum potential energy where a water molecule is trapped near the CNT edge using the velocity Verlet method at the temperature of 0 K. A water molecule is located at the outlet of the CNT in the initial configuration. After the steps corresponding to 3 ns, the water molecule reaches about 0.6 nm inside from the CNT edge. The binding energy between the CNT and water is determined to be 2.4×10^{-20} J. In order to determine the binding energy between water molecules, we first conducted the similar energy minimization for the system of two water molecules in vacuum. The binding energy for these two water molecules, i.e., the energy of hydrogen bond for an isolated pair of the water molecules, is 5.0×10^{-20} J. Then, we have also calculated the binding energy using the configuration of two water molecules inside the CNT. The obtained binding energy was 5.0×10^{-20} J. Thus, among the two components of the binding energy between the water cluster and the outlet region, the contribution from the water chain that is connected from inside the CNT is stronger than that from the CNT itself. These values are presumably the maximums of the possible configurations in the jet dynamics because the presence of many other molecules limits the available configuration in the actual process.

We have also conducted quantum-mechanical (QM) calculation to confirm the applicability of the classical potential used here to such consideration. GAUSSIAN03 [42] is used for the QM calculations. Locating two water molecules in a (6,6) CNT with unit length of 0.49 nm corresponding to 48 carbon atoms [22], energy minimization is conducted with Hartree Fock using basis set of STO-3G under the condition of fixed carbon atoms and periodic boundary condition in the tube axis direction. Then, the energy minimization is continued using the density-functional theory with B3LYP and the basis set 3–21G(d) in order to improve the precision. The structure of minimum energy for the entire system is thus obtained (cf. Ref. [22] for the detail of the initial and final structures). The

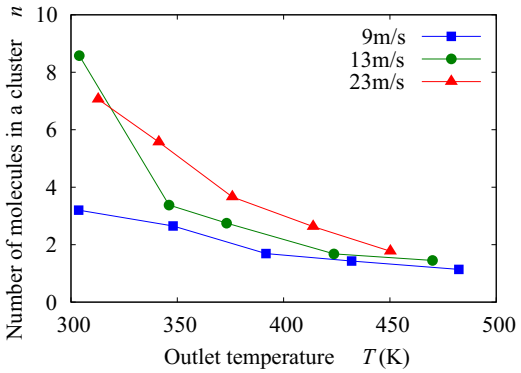

FIG. 3. (Color online) Size of water clusters released from the outlet.

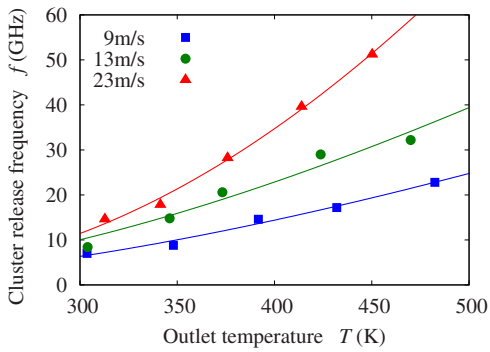

FIG. 4. (Color online) Release frequency of water clusters from the outlet. The solid lines indicate the fitted curve based on Eq. (8).

configuration is then used entirely or partly for the calculation of binding energies. Denoting the energy of the entire structure consisting of the CNT and two water molecules by $E_{\text{CNT-2H}_2\text{O}}$ and those of the isolated CNT, and the set of two water molecules, respectively, by E_{CNT} and $E_{2\text{H}_2\text{O}}$, the binding energy $\Delta E_{\text{CNT-H}_2\text{O}}$ between the (6,6) CNT and a confined water molecule can be calculated as

$$\Delta E_{\text{CNT-H}_2\text{O}} = \frac{1}{2}[(E_{\text{CNT}} + E_{2\text{H}_2\text{O}}) - E_{\text{CNT-2H}_2\text{O}}]. \tag{5}$$

Consequently, $\Delta E_{\text{CNT-H}_2\text{O}} = 1.1 \times 10^{-20}$ J.

Similarly, the hydrogen-bond energy $\Delta E_{\text{H}_2\text{O-H}_2\text{O}}$ between the two water molecules confined in the (6,6) CNT can be calculated. Denoting the energy of the hydrogen-bonded pair of the water molecules "A" and "B" by E_{AB}, and those of the isolated water molecules by E_{A} and E_{B}, the hydrogen-bond energy is

$$\Delta E_{\text{H}_2\text{O-H}_2\text{O}} = (E_{\text{A}} + E_{\text{B}}) - E_{\text{AB}}. \tag{6}$$

The calculation is conducted for the two hydrogen bonds due to the periodic boundary condition [22], and the obtained value was 8.4×10^{-20} J in both cases. Thus, the trend that the binding energy between water molecules is substantially larger is in good agreement with that of the classical MD potential. The difference between $\Delta E_{\text{H}_2\text{O-H}_2\text{O}}$ and $\Delta E_{\text{CNT-H}_2\text{O}}$ is larger for QM than the force field used in this study. In particular, the smaller $\Delta E_{\text{H}_2\text{O-H}_2\text{O}}$ for the classical MD than for the QM is mainly attributed to the shifted-force truncation of the electrostatic interactions. Nevertheless, the order of the energies is the same with QM. Therefore, we consider that the qualitative discussion on the result in this paper is valid.

B. Jet properties and role of thermal fluctuations

The dependence of the size and release frequency of a water cluster on the temperature and streaming velocity is shown in Figs. 3 and 4. The event of cluster release is dominated by the thermal fluctuations of the water molecules at the outlet. When the temperature is higher, there is higher probability that the cluster gets the kinetic energy larger than the binding energy to the outlet. Therefore, the clusters tend to be released earlier at higher temperatures, which means having shorter time to grow with the same flow rate. Consequently, the cluster size decreases with increasing temperature. Correspondingly, the release frequency of the cluster increases with the temperature. Because of the mass conservation, the following relation holds:

$$\rho_{N/L} u_{\text{out}} = nf, \tag{7}$$

where $\rho_{N/L}$, n, and f are the number density of water molecules per unit length of the CNT at the outlet, the number of water molecules in a cluster getting released, and the release frequency. However, the data in Figs. 3 and 4 do not exactly match because of the sampling limitation including the fact that some clusters split after the release from the outlet.

If f is dominated by the bond-breaking process, it is reasonable to assume that the temperature dependence roughly follows the transition state theory of reaction kinetics, i.e., $f \propto k_{\text{TST}}$, where k_{TST} is the rate constant. The fitting of the following equation

$$f(T) = CT \exp\left(-\frac{\Delta E}{k_B T}\right), \tag{8}$$

to the measured data are also plotted in Fig. 4, where T is the temperature, and both C and ΔE were employed as the fitting parameters. The curves fit well to the simulation results. The ΔE for the three lines are roughly around 1×10^{-20} J, which is smaller than $\Delta E_{\text{cluster-chain}}$ discussed above. Although they cannot be directly compared because C is also the fitting parameter, one of the reason is that the $\Delta E_{\text{cluster-chain}}$ defined in the previous section is based on the isolated pair of water molecules at 0 K, which leads to the evaluation of the deeper well of the potential energy due to the absence of other molecules that limits the possible configuration.

The outlet streaming velocity itself does not directly contribute to the unbinding of a cluster from the water chain in the (6,6) CNT. This is because the cluster velocity in time average is smaller than the single-file chain in the CNT as a consequence of mass conservation with the widening cross section of the working fluid. In other words, the upstream molecules "catch up" the cluster. In order for the cluster to be released from the chain, the instantaneous velocity of the cluster needs to be larger than the following chain. The magnitude of the difference needs to be large enough so that the

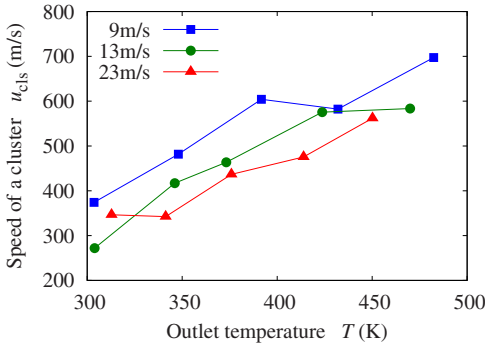

FIG. 5. (Color online) Speed of water clusters released from the outlet.

corresponding kinetic energy is larger than the binding energy between the cluster and the chain. Nevertheless, the release frequency is larger for higher streaming velocities. Although the streaming velocity does not contribute to the unbinding of the cluster from the water chain, the difference of the streaming velocity can affect the unbinding of water from the CNT fixed in space and contributes partly to the release from the outlet region. In particular, it is the only binding energy to overcome when the water chain is already ruptured in the (6,6) CNT. On the other hand, the cluster size becomes larger when the streaming velocity is higher since more water molecules are supplied per unit time. Although the temperature dependence of cluster size and release frequency is a complementary information at the same streaming velocity, this is not the case for the dependence on the streaming velocity at the same temperatures.

The speed of the released water clusters is shown in Fig. 5 as a function of temperature. The speed of the cluster increases with temperature but the increase in outlet streaming velocity does not lead to it. This property is rather directly related to the cluster size, which is shown in Fig. 6. Both higher temperatures and lower streaming velocities lead to smaller cluster size. It can be clearly seen that the smaller water clusters have higher speeds. This is because the speed of a released cluster is determined by the instantaneous mean velocity of the cluster just unbound from the outlet. The cluster velocity $\boldsymbol{u}_{\mathrm{cls}}$ is the total of the outlet streaming velocity $\boldsymbol{u}_{\mathrm{out}}$ and the instantaneous ensemble average $\langle \boldsymbol{v}' \rangle$ of the thermal velocities of the constituent atoms:

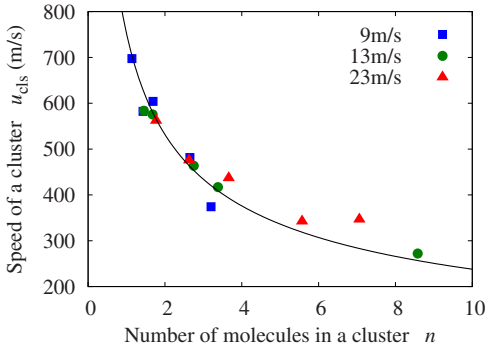

FIG. 6. (Color online) Relation between the speed and size of water clusters. The solid line indicates the fitted curve $\boldsymbol{u}_{\mathrm{cls}}=cn^{-1/2}$, where c is the fitting parameter, based on Eqs. (9) and (11) with the assumption of $|\boldsymbol{u}_{\mathrm{out}}| \ll |\boldsymbol{v}'|$.

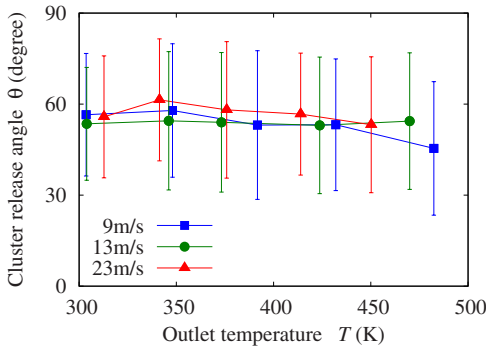

FIG. 7. (Color online) Release angle of water clusters from the outlet. The 0° corresponds to the angle along the tube axis. The error bars indicate the standard deviations.

$$\boldsymbol{u}_{\mathrm{cls}} = \boldsymbol{u}_{\mathrm{out}} + \langle \boldsymbol{v}' \rangle, \tag{9}$$

$$\langle \boldsymbol{v}' \rangle \equiv \frac{\sum_{i=1}^{n} m_i \boldsymbol{v}_i'}{\sum_{i=1}^{n} m_i}, \tag{10}$$

where m_i and $\boldsymbol{v}_i'$ are the total number of atoms in the cluster getting released, mass, and thermal velocity of the atom i, respectively. The $\langle\ \rangle$ of $\langle \boldsymbol{v}' \rangle$ here stands for the instantaneous ensemble average in the cluster. The average thermal velocities of water molecules at ambient or higher temperatures are much higher than the streaming velocity discussed in this paper. The root-mean-square thermal velocity of a water molecule at 300 K is 644 m/s. Hence, $\boldsymbol{u}_{\mathrm{cls}}$ is dominated by the thermal velocities owing to the small size of the cluster. The speed of a cluster is much higher than the outlet streaming velocity (cf. Fig. 5) although it is somewhat lower than the thermal velocity of a single molecule because of the averaging [Eq. (10)]. Furthermore, the probability of having larger value for $\langle \boldsymbol{v}' \rangle$ is higher for smaller clusters due to the central limit theorem, i.e.,

$$\langle \boldsymbol{v}' \rangle \propto \frac{1}{\sqrt{n}}. \tag{11}$$

This is because $\langle \boldsymbol{v}' \rangle$ is the average of the *thermal* velocities, i.e., the standard deviation component by definition. Therefore, the smaller clusters tend to have higher speeds. The approximation $\boldsymbol{u}_{\mathrm{cls}} \approx cn^{-1/2}$, where c is a coefficient for fitting, with the assumption $|\boldsymbol{u}_{\mathrm{out}}| \ll |\boldsymbol{v}'|$ matches the simulation results very well.

Figure 7 shows the spread angle of the water clusters as a function of the temperature. Although the speed depends on the temperature, the release angle looks independent of them. The angle is roughly around in the range from 50° to 60° from the tube axis. This is because the angle is mainly determined by the thermal velocity. The thermal velocity is isotropic since the extent of nonequilibrium is not extreme, i.e., the root-mean-square thermal velocity in each direction v_x', v_y', and v_z' holds $v_x'=v_y'=v_z'$. Consequently, there is no substantial preference on the orientation. Indeed, the ap-

proximate spread angle θ can be estimated as follows:

$$\cos\theta \approx \frac{v_z'}{\sqrt{v_x'^2 + v_y'^2 + v_z'^2}} = \frac{1}{\sqrt{3}}, \tag{12}$$

where the last equality is due to the isotropy. Thus, $\theta = \cos^{-1}(1/\sqrt{3}) \approx 55°$, which is in good agreement with Fig. 7. It should be noted that the sampling region of the cluster does not cover the upstream side from the outlet.

These jet properties make a great contrast with macroscopic atomization phenomena by Kelvin-Helmholtz instability, where higher streaming velocity leads to smaller droplet size due to the interfacial wave growth with small wavelength. The dominant factor of this nanojet breakup mechanism is the thermal fluctuations relative to the binding energy between the water cluster and the outlet region, whereas it is the Weber number, i.e., the fluid's inertia relative to the interfacial tension, for the macroscopic corresponding system.

IV. CONCLUDING REMARKS

We have conducted the molecular-dynamics simulations to elucidate the properties of nanojet from a (6,6) CNT, where water molecules are supplied from the upstream in a single-file manner. The results show the characteristics qualitatively different from the macroscopic liquid jets that are dominated by the Kelvin-Helmholtz instability. The role of thermal fluctuations is dominant in the intermittent release of water clusters formed at the outlet. The consequent strong temperature dependence indicates that the effective control of the nanojet is to be realized by the utilization of thermal fluctuations, rather than the suppression of it as a noise.

[1] M. Moseler and U. Landman, Science **289**, 1165 (2000).
[2] J. Eggers, Phys. Rev. Lett. **89**, 084502 (2002).
[3] T.-H. Fang, W.-J. Chang, and S.-C. Liao, J. Phys.: Condens. Matter **15**, 8263 (2003).
[4] Y. S. Choi, S. J. Kim, and M.-U. Kim, Phys. Rev. E **73**, 016309 (2006).
[5] S. Murad and I. K. Puri, Nano Lett. **7**, 707 (2007).
[6] J. Voigt, B. Reinker, I. W. Rangelow, G. Mariotto, I. Shvets, P. Guethner, and H. Löschner, J. Vac. Sci. Technol. B **17**, 2764 (1999).
[7] J. Voigt, F. Shi, P. Hudek, I. W. Rangelow, and K. Edinger, J. Vac. Sci. Technol. B **18**, 3525 (2000).
[8] I. W. Rangelow, J. Voigt, and K. Edinger, J. Vac. Sci. Technol. B **19**, 2723 (2001).
[9] F. Song, M. Han, M. Liu, B. Chen, J. Wan, and G. Wang, Phys. Rev. Lett. **94**, 093401 (2005).
[10] S. Iijima, Nature (London) **354**, 56 (1991).
[11] S. Iijima and T. Ichihashi, Nature (London) **363**, 603 (1993).
[12] M. C. Gordillo and J. Martí, Chem. Phys. Lett. **329**, 341 (2000).
[13] K. Koga, G. T. Gao, H. Tanaka, and X. C. Zeng, Nature (London) **412**, 802 (2001).
[14] T. Werder, J. H. Walther, R. L. Jaffe, T. Halicioglu, F. Noca, and P. Koumoutsakos, Nano Lett. **1**, 697 (2001).
[15] J. Rivera, C. McCabe, and P. T. Cummings, Nano Lett. **2**, 1427 (2002).
[16] J. H. Walther, R. Jaffe, T. Halicioglu, and P. Koumoutsakos, J. Phys. Chem. B **105**, 9980 (2001).
[17] J. Martí and M. C. Gordillo, J. Chem. Phys. **114**, 10486 (2001).
[18] R. J. Mashl, S. Joseph, N. R. Aluru, and E. Jakobsson, Nano Lett. **3**, 589 (2003).
[19] J. Wang, Y. Zhu, J. Zhou, and X.-H. Lu, Phys. Chem. Chem. Phys. **6**, 829 (2004).
[20] G. Hummer, J. C. Rasaiah, and J. P. Noworyta, Nature (London) **414**, 188 (2001).
[21] I. Hanasaki and A. Nakatani, J. Chem. Phys. **124**, 174714 (2006).
[22] I. Hanasaki, A. Nakamura, T. Yonebayashi, and S. Kawano, J. Phys.: Condens. Matter **20**, 015213 (2008).
[23] S. C. Kassinos, J. H. Walther, E. Kotsalis, and P. Koumoutsakos, Lect. Notes Comput. Sci. **39**, 215 (2004).
[24] E. M. Kotsalis, J. H. Walther, and P. Koumoutsakos, Int. J. Multiphase Flow **30**, 995 (2004).
[25] I. Hanasaki and A. Nakatani, J. Chem. Phys. **124**, 144708 (2006).
[26] J. K. Holt, H. G. Park, Y. Wang, M. Stadermann, A. B. Artyukhin, C. P. Grigoropoulos, A. Noy, and O. Bakajin, Science **312**, 1034 (2006).
[27] J. Koplik, Phys. Fluids A **5**, 521 (1993).
[28] S. Kawano, Phys. Rev. E **58**, 4468 (1998).
[29] D. Min and H. Wong, Phys. Fluids **18**, 024103 (2006).
[30] H. J. C. Berendsen, J. R. Grigera, and T. P. Straatsma, J. Phys. Chem. **91**, 6269 (1987).
[31] U. Zimmerli, P. Gonnet, J. H. Walther, and P. Koumoutsakos, Nano Lett. **5**, 1017 (2005).
[32] J. H. Walther, T. Werder, R. L. Jaffe, and P. Koumoutsakos, Phys. Rev. E **69**, 062201 (2004).
[33] I. Hanasaki, A. Nakamura, T. Yonebayashi, and S. Kawano, J. Phys.: Condens. Matter **20**, 015213 (2008).
[34] S. Andreev, D. Reichman, and G. Hummer, J. Chem. Phys. **123**, 194502 (2005).
[35] S. Jakobtorweihen, M. G. Verbeek, C. P. Lowe, F. J. Keil, and B. Smit, Phys. Rev. Lett. **95**, 044501 (2005).
[36] S. Iijima, T. Ichihashi, and Y. Ando, Nature (London) **356**, 776 (1992).
[37] R. Saito, G. Dresselhaus, and M. S. Dresselhaus, Phys. Rev. B **53**, 2044 (1996).

[38] I. Hanasaki and A. Nakatani, Nanotechnology **17**, 2794 (2006).
[39] I. Hanasaki and A. Nakatani, Modell. Simul. Mater. Sci. Eng. **14**, S9 (2006).
[40] J. Martí, J. Chem. Phys. **110**, 6876 (1999).
[41] W. Humphrey, A. Dalke, and K. Schulten, J. Mol. Graphics **14**, 33 (1996).
[42] M. J. Frisch *et al.*, GAUSSIAN 03 Revision C02, Gaussian, Inc., Wallingford, CT (2004).
[43] H. C. Andersen, J. Comput. Phys. **52**, 24 (1983).